International Journal of Applied Pharmaceutics

ISSN- 0975-7058 Vol 18, Issue 3, 2026

Original Article

IN VITRO CYTOTOXICITY AND WOUND HEALING EFFICACY OF BIOSYNTHESIZED SILVER NANOPARTICLES FROM *AGERATINA ADENOPHORA* AQUEOUS STEM EXTRACT

LISHANTHI RAVI, LORRAINE V. MARY ROCHA, MADEENA S. BEGUM, HADSUN A. JONA, JAQULINE CHINNA RANI I.*

Department of Plant Biology and Biotechnology and Loyola Institute of Frontier Energy (LIFE), Loyola College (Autonomous), University of Madras, Chennai, Tamil Nadu, India

***Corresponding author: Jaqueline Chinna Rani I.; *Email: jaqulinecr@loyolacollege.edu**

Received: 17 Oct 2025, Revised and Accepted: 06 Mar 2026

ABSTRACT

Objective: The present study was aimed to synthesize biogenic silver nanoparticles (AgNPs) from *Ageratina adenophora (A. adenophora)* aqueous stem extract and also to study its antimicrobial, antioxidant, cytotoxic and enhanced wound healing properties on Vero cell line.

Methods: The biogenic AgNPs were synthesized using aqueous stem extracts of *A. adenophora* and were characterized using ultraviolet-visible spectroscopy, High-resolution transmission electron microscopy (TEM), X-ray diffraction (XRD) and Fourier-transform infrared spectroscopy (FTIR). The AgNPs were tested for their antibacterial and antifungal efficacy using the agar well diffusion method. The DPPH scavenging ability of AgNPs was studied, and MTT assay was used to evaluate the cytotoxic effects and wound scratch assay was performed to study the potential healing activity of biosynthesized AgNPs on vero cells.

Results: AgNPs synthesized using *A. adenophora* aqueous stem extract showed good stability, with maximum absorption spectra of 450 nm. The synthesized AgNPs were found to be spherical in shape with a size range between 20-60 nm. The XRD indicates that the crystalline structure of AgNPs is a face-centred cubic (fcc) crystal. The AgNPs showed good stability and scavenging activity. The Vero cell line at lower concentrations display acceptable biocompatibility for AgNPs with IC_{50} concentration of 108.61 µg/ml, indicating concentration-dependent cytotoxicity *in vitro*. The synthesised AgNPs demonstrated 57.97 % wound closure rate, indicating substantial potential for wound healing.

Conclusion: According to the results, the synthesized AgNPs using aqueous stem extract of *A. adenophora* has demonstrates effective wound healing potential on Vero cell lines.

Keywords: Silver nanoparticles, Antimicrobial, Antioxidant, Cytotoxicity and Wound healing

DOI: https://dx.doi.org/10.22159/ijap.2026v18i3.57193 Journal homepage: https://innovareacademics.in/journals/index.php/ijap

INTRODUCTION

Nanotechnology is a fast-evolving domain with fabrication of nanomaterials at its forefront. Particles less than 100 nm are generally referred to as nanoparticles. Their unique size makes them superior and indispensable in various applications [1]. Science and technology research in nanotechnology promises breakthroughs in areas such as materials and manufacturing, medicine, health care, energy, biotechnology [2] and in combating microbes, drug delivery, treatment of environmental waste, and treatment of chronic disease [3]. Green synthesis aids in the reduction of metal salts to nanoparticles. The most straightforward method for producing green nanoparticles is to employ biological resources including microbes, plants, or their components [4]. A wide range of microorganisms and plants have been investigated so far and proven effective in the creation of green nanoparticles. Nanoparticles made from plants are biocompatible and very stable, as plants contain phytochemicals, which may function as capping and reducing agents, easing the synthesis process [5].

Among all metallic nanoparticles, silver (Ag) nanoparticles have received the most attention due to their distinctive features and environmental friendliness. Silver nanoparticles created using green synthesis technology are outstanding in terms of their physicochemical properties, making them non-toxic and minimising adverse effects [6]. Both the physical and chemical ways of making AgNPs are more energy-intensive and cost-effective. It is commonly acknowledged that AgNPs have positive effects upon the antioxidant, antidiabetic, cytotoxic, antimicrobial, fungicidal, and anti-inflammatory effects, in addition to many other potential uses [7]. In recent times, biosynthesis of AgNPs has been explored using *Panax ginseng, Datura metel, Acalypha indica, Lantana camara, and Camellia sinensis* , which have been used to synthesize AgNPs with interesting potential biomedical applications [8, 9].

Ageratina adenophora S. R. King and H. Rob is an invasive plant native to Mexico that belongs to the Asteraceae family. The plant has been used in traditional medicine for the treatment of skin diseases, wounds, inflammation, diabetes and fever. *A. adenophora* has been the subject of various research, which has recorded and isolated a large number of secondary metabolites [10]. It is well known to contain a variety of bioactive phytochemicals, including saponins, carbohydrates, phenolic compounds, alkaloids, flavonoids and terpenoids [11]. Pharmacological research has shown a wide range of biological potential, including prospective uses for antidiabetic, antioxidant, antimicrobial, fungicidal, and anti-inflammatory properties [12]. While additional research has established that some of the euptox pharmacological features have focused only on the adverse effects of the toxin. Despite being toxic, *A. adenophora* has certain isolated secondary metabolites that have helped researchers develop novel strategies to utilise its safe medicinal properties. According to previous reports, the phytochemicals present in the invasive plant *A. adenophora* have been studied for their effective wound-healing activity [13].

The current work aimed to use *A. adenophora* aqueous stem extract for the green synthesis of AgNPs for the first time, as per our knowledge. Further, characterization analysis was done by using ultraviolet–visible spectroscopy (UV–Vis), Fourier transform infrared spectroscopy (FTIR), High-resolution transmission electron microscopy (HR-TEM) and X-ray diffraction (XRD) to confirm their optical properties, functional groups involved in synthesis, morphology and crystalline structure. Moreover, biological activities were performed against pathogenic bacteria and fungi to evaluate its antimicrobial activity. Furthermore, biosynthesized nanoparticles were also studied for their antioxidant activity, wound healing property and cytotoxic effect on Vero cell line under *in vitro* conditions.

MATERIALS AND METHODS

Chemicals and reagents

All chemicals and reagents used were of analytical grade and purchased from Sigma Aldrich Co. (St Louis, MO, USA). Silver nitrate ($AgNO_3$), Bovine Serum (FBS), Cell culture Dulbecco's Modified Eagle Medium (DMEM) and 0.25% trypsin-EDTA were obtained from Himedia Laboratories Private Limited, Mumbai, India. Streptomycin, penicillin, distilled water dimethyl sulfoxide (DMSO), (3-(4, 5-dimethylthiazol-2-yl)-2,5-diphenyltetrazolium bromide) (MTT), Nutrient agar (NA) agar/broth and phosphate buffer were purchased from Sigma-Aldrich (St Louis, MO, USA).

Plant material collection

The healthy plants of *Ageratina adenophora* (Spreng.) R. King and H. Rob were collected in and around Kairbetta Hosahatti, Kotagiri, during March 2023. The plant components were validated and taxonomically authenticated by Siddha Central Research Institute, Chennai Code (A19042304A).

Preparation of *Ageratina adenophora* stem extract

The fresh aerial parts of *A. adenophora* were washed with tap water and then rinsed with distilled water to get rid of water-soluble contaminants and loosely adherent particles. The stem samples were shade-dried for two weeks to eliminate humidity and then ground to a coarse powder using a blender. In the current study, 4 g of powder was taken and mixed with 100 ml of distilled water in a glass beaker, and kept in a water bath for 20 min at 60 °C. After cooling, the aqueous stem extract of *A. adenophora* was filtered with Whatman No. 1 filter paper and stored in an amber bottle at 4 °C to avoid direct sunlight. Then the aqueous extract was used for the preparation of nanoparticles, phytochemical analysis and further characterization, and biological studies [14].

Synthesis of silver nanoparticles

During preliminary screening, $AgNO_3$ of different concentrations (10, 20, 40, 60 mmol and 1 M) was used for the synthesis of nanoparticles and the optimum concentration of silver ion (1M $AgNO_3$) was determined based on maximum UV absorption spectroscopy. To biosynthesize AgNPs, an aqueous solution of silver nitrate ($AgNO_3$:1 mmol) was prepared. For the synthesis process, 1 ml of *A. adenophora* aqueous stem extract was added to 9 ml of silver nitrate solution (1 mmol). To reduce the photoactivation of silver nitrate, the reaction was carried out overnight at room temperature in the dark. A shift from pale yellow to dark brown in visual appearance indicated the formation of AgNPs. The solution mixture was centrifuged for 10 min at 9,000 rpm and purified using double-distilled water. The process was repeated three times. A control setup was also maintained with the aqueous stem extracts of *A. adenophora* and $AgNO_3$ solution. UV-Visible spectroscopy was used to confirm the synthesized AgNPs, and changes in the variables were recorded [14].

Physicochemical characterization of AgNPs

UV–visible spectroscopy and stability analysis

UV-Visible True Double Beam Spectrophotometer (UV PLUS Desktop Model-Motras Scientific) was used to measure the optical properties of AgNPs between 300 nm and 700 nm range using PC based spectroscopic spectra. The UV–Visible spectra of the aqueous stem extract and silver nitrate solution were also recorded, which showed no peaks. The stability of AgNPs was also recorded at different time intervals (12 h, 24 h, 5^{th} d, 15^{th} d, 30^{th} d and 60^{th} d) [15].

Fourier transform infrared spectroscopy (FTIR) analysis

To determine the unique functional groups in the biogenic AgNPs, FTIR analysis was performed using BRUKER Optik GmbH (MODEL No-TENSOR 27, SOFTWARE-OPUS version 6.5), and recorded in the wavenumber range of 400 to 4000 cm^{-1}. For comparison, FTIR spectral analysis was performed on the aqueous stem extract and synthesized AgNPs of *A. adenophora*. The biomolecules responsible for reducing and stabilizing the silver nanoparticles were identified using FTIR measurements. The FTIR peak values were recorded twice to ensure accuracy and reliability of the readings [16].

X-ray diffraction (XRD) analysis

X-ray diffraction (XRD) analysis was performed to identify and evaluate the structural properties of the silver nanoparticles synthesized using green methods. The AgNPs coated on the XRD grid were examined using the Empyrean X-ray diffractometer model, running at 40 kV and 35 mA current, with CuKα radiation of wavelength 1.5406 Å. The crystalline size of AgNPs was determined through the XRD pattern measured over a 2θ range from 35° to 70° with a step size of 0.04° per second [17]. The size of the AgNPs was determined by Scherrer's formula, given as follows:

$$D = k\lambda/\beta\cos\theta$$

where D is the particle size (nm), k is a constant, λ is the X-ray wavelength, β is the full line width at half maximum (FWHM) elevation of the important peak, and θ is the Bragg's diffraction angle.

High-resolution transmission electron microscopy (HR-TEM) analysis

The morphological structure of AgNPs, including their size, shape and structure, was determined using TEM analysis. On copper grids covered with carbon, a drop of synthesized AgNPs was applied. Blotting paper was used to remove any extra solution after it had stood for 2 min and it was then allowed to dry at room temperature. Jeol/JEM-2100 instrument accelerating at 200 kV was used to carry out transmission electron microscopy studies [18].

Dynamic light scattering (DLS) analysis

Dynamic light scattering (DLS) is a significant method used to investigate the size distribution of biosynthesized nanoparticles that exist within a solution. The phase behavior of the nanoparticles was assessed using the Nano Plus particle size analyzer instrument. The measurements were taken at 90° angle, and an average temperature of 25 °C was maintained. The silver nanoparticle suspension was sonicated in distilled water for 5 min. The polydispersity index (PDI), which is the ratio of the weight average, was calculated. The normal range of PDI value was between 0.05 and 0.7, while a value beyond 0.7 indicates an undesirable broad particle size distribution [7, 16].

Preliminary phytochemical analysis of *Ageratina adenophora* stem extract

Ageratina adenophora aqueous stem extract was subjected to a qualitative phytochemical screening process using standard procedures. The outcome was noticed by a change in colour. The qualitative phytochemical screening revealed the existence of alkaloids, carbohydrates, flavonoids, proteins, amino acids, phenols, saponins, steroids, and terpenoid compounds [19].

Quantitative phytochemical analysis

Aqueous stem extract of *A. adenophora* was used to quantify phytochemicals. The total phenol content (TPC) was determined by the standard Folin-Ciocalteau (F–C) method. The reagent (F–C) is sensitive to reducing compounds, forming a blue colour complex. UV-visible spectrophotometer absorbance was measured at 650 nm for the sample, and gallic acid was used as a standard (1 mg/ml). The total phenolic content (TPC) was calculated from the standard curve, and the results were expressed as gallic acid equivalent (mg/g of extracted compound) [20]. Total flavonoid concentration (TFC) was determined using a modified calorimetric method. Following the protocol, the alkaloid content was determined. The absorbance was measured at 510 nm. A standard calibration curve was prepared with standard quercetin (1 mg/ml) in deionised water. The total flavonoid content (TFC) was calculated, and the results were expressed as quercetin equivalents (mg/g of extracts) [21]. The total alkaloid content (TAC) was determined by following the standard protocol with slight modification by the spectrophotometer method [22]. The absorbance was measured at 470 nm. The quantitative experiment was conducted in triplicate.

Determination of free radical scavenging activity – DPPH assay

The DPPH scavenging ability of AgNPs was determined according to Rajamanikandan *et al.* [23]. Various concentrations (20, 40, 60, 80, and 100 µg/ml) of biogenic AgNPs was mixed with the methanolic DPPH working solution of 2 ml concentration. Methanolic DPPH reagent without silver nanoparticles was used as a control and ascorbic acid was used as a standard [24]. The mixture was shaken and incubated in a dark condition for 20 min at room temperature. The radical scavenging activity was measured at 517 nm using a UV-Visible spectrophotometer against methanol as a blank. The inhibition (%) was calculated using the following equation, with a lesser IC_{50} value indicating stronger antioxidant capacity:

$$\text{Inhibition } \% = [(A_{\text{control}} - A_{\text{sample}}) / A_{\text{control}}] \times 100$$

where $A_{control}$ was the absorbance of control (blank, without samples) and A_{sample} was the absorbance in the presence of the sample. All the tests were done in triplicate, and the mean values were used to plot the graph from which the IC_{50} values (µg/ml) were determined. Here IC_{50} value is the effective amount of test samples needed to scavenge DPPH radical by 50%.

Antibacterial activity of synthesized AgNPs

Agar well diffusion method was used to study the antibacterial activities of the biogenic AgNPs. Gram-positive bacteria *Bacillus subtilis*, *Staphylococcus aureus* and Gram-negative bacteria *Escherichia coli*, *Pseudomonas aeruginosa* were used as test pathogens. The bacterial pathogens were freshly cultured in the nutrient broth for 24 h, and the pathogens were spread on the medium plates and four wells of 6 mm diameter were made using a sterile cork borer. During preliminary screening, AgNPs of different concentrations (20, 40, 60, 80 and 100 µl**) were evaluated to test the pathogens and the optimum concentration was finalized to 80 µl** and 20 µl** of 10 µg positive control gentamicin based on earlier reports [25]. The synthesized AgNPs were loaded in well A, aqueous stem extract in well B, $AgNO_3$ (1 mmol) in well C with a concentration of 80 µl** and 20 µl** of 10 µg positive control gentamicin concentration in well D, and the plates were incubated for 24 h at 37 °C. The zone of inhibition (ZOI; mm) was measured for antibacterial activity.

Antifungal activity of synthesized AgNPs

The antifungal activity of the biogenic AgNPs was investigated using the agar well diffusion technique. Fungal pathogens *Aspergillus niger* and *Candida albicans* were inoculated in potato dextrose agar (PDA) media. In the petri plate, the samples were loaded into four wells of 6 mm diameter. The synthesized AgNPs were loaded in well A, aqueous stem extract in well B, $AgNO_3$ (1 mmol) in well C with a concentration of 80 µl** and 20 µl** of 10 µg positive control clotrimazole in well D and the plates were incubated for 24 h at 37 °C. The zone of inhibition was recorded [25, 7].

Minimal inhibitory concentration (MIC)

The MIC of the AgNPs was determined according to the methodology of Sengupta *et al.* [26] using the broth microdilution method. The selected strains of bacterial suspensions. (*E. coli, P. aeruginosa, B. subtilis and S. aureus*) were prepared and added to Muller-Hinton broth (MHB) cultures. Then two-fold dilutions of different concentrations of AgNPs (1.25 to 10 mg/ml) were loaded into the respective wells and incubated at 37 °C for 16 to 24 h. The absorbance was measured at 600 nm to obtain the MIC, and the values were recorded for all the triplicates. The MIC is the lowest dose of AgNPs at which bacteria impedes 90% of growth.

***In vitro* cytotoxicity of synthesized AgNPs on vero cell line (MTT assay)**

MTT assay was used to evaluate the cytotoxic effects of biogenic AgNPs on Vero cells [27]. 96-well microplates were used to seed Vero cells and they were cultured for 48 h at 37 °C with 5% CO_2 to promote 90% of cell growth under the optimum conditions. The cells were treated with different concentrations of biogenic AgNPs (10, 20, 40, 60, 80 and 100 µg/ml) and they were incubated for 24 h. The non-treated cells were marked as control. After 24 h of incubation, the medium was removed, and the cells were washed with PBS. The treated cells were subjected to a concentration of 20 µL of MTT solution and incubated for 2 h at 37 °C in dark. The blue formazan crystals that formed were dissolved in 100 µL of DMSO. An ELISA microplate reader was used to measure the absorbance at 570 nm. The morphological alterations of untreated (control) and treated cells were examined. The cell viability percentage was calculated using the formula:

$$\text{Cell Viability } (\%) = (\text{Absorbance of treated cells}/\text{Absorbance of control cells}) \times 100$$

***In vitro* wound healing activity of synthesized AgNPs**

The experiment was performed according to the standardised protocol and previous reports [28, 29]. Vero cells were seeded in a 6-well plate and grown under optimum conditions until they attained a 90–95% confluence. A P10 pipette tip was used to create a wound-like scratch in the middle of the cell monolayer, and the cell debris was then washed away with new media. The wound was exposed to synthesized AgNPs with a concentration of 50 µg/ml in a humidified environment containing 5% CO_2 at 37 °C for 24 to 48 h. The negative control cells were not given any treatment, and cipladine was used as a positive control with 50 µg/ml concentration. The study of scratch wound closure was analysed by taking digital images under the digital inverted microscope at different time intervals: 0 h ($t0$), 24 h ($t1$), and 48 h ($t2$). By evaluating the difference between the wound widths at $t0$, $t1$ and $t2$, using the Image J processing software, the scratch's closure was noted as described by Felice *et al.* [29]. Scratch closure rate (SCR) was calculated using the formula:

$$SCR = [(At0 - At) / At0] \times 100$$

where A*t*0 is the scratch area at time 0, and A*t* is the scratch area at 24 h and 48 h.

RESULTS

Biosynthesis of AgNPs

The biological reduction approach used to synthesize AgNPs from *A. adenophora* aqueous stem extract exhibited a change in color from pale yellow to dark brown was observed in the test sample (T) when compared to the control (C), as shown in fig. 1b. Along with good stability, indicating the formation of nanoparticles. The phytochemicals in the plant are responsible for the formation of AgNPs by causing the surface plasmon resonance excitation effect, which is linked to the various color changes of silver nanoparticles [30].

Characterization of AgNPs

The biologically synthesized AgNPs nanoparticles were characterized using various techniques, including ultraviolet–visible spectroscopy (UV–Vis), Fourier transform infrared spectroscopy (FTIR), High-resolution transmission electron microscopy (HR-TEM), Particle size analysis and X-ray diffraction (XRD).

UV– visible spectroscopy and stability analysis

The UV-Visible True Beam Spectrophotometer (UV PLUS Motras Scientific) was used to examine the optical properties of AgNPs. The change in color due to the excitation of surface plasmon resonance (SPR) in metal nanoparticles. The SPR displayed a wavelength peak at 430 nm following a 12 h incubation period. The peak moved to 450 nm after 24 h and remained stable for two months (fig. 2a). UV-visible spectra analysis was used to evaluate the stability of the synthesized AgNPs at regular time intervals (12 h, 24 h, 5thday, 15thday, 30thday, and 60th day), with wavelengths ranging from 300 to 700 nm as shown in (fig. 2b). The $AgNO_3$ solution and *A. adenophora* aqueous stem extract alone did not show any peaks. The results align with previous studies reporting SPR peaks for green synthesized AgNPs with good stability using plant extract [25, 31].

Fig. 1: a) Aerial part of *A. adenophora* in its natural habitat, b) Biosynthesis screening of AgNPs from *Ageratina adenophora* stem extract

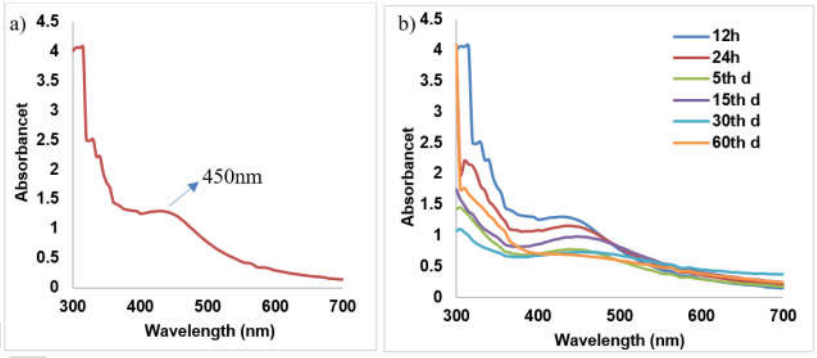

Fig. 2: (a) UV–vis spectra of AgNPs and (b) Stability spectra of AgNPs at different time durations . Abbreviations: h (n=6)

Fourier transform infrared spectroscopy

The interaction of AgNPs with the functional groups of aqueous stem extract of *A. adenophora* was analyzed by FTIR analysis. For comparative study, FTIR spectra analysis of *A. adenophora* stem extract, both before and after the formation of AgNPs, was performed to identify the functional groups responsible for nanoparticle production. In this study, the FTIR spectra for the stem extract, displayed several prominent peaks at 1121, 1384, 1595, 2929, 3438 cm^{-1} as shown in (fig. 3a). A broader peak at 3,438 cm^{-1} due to the stretching of the hydroxyl functional group in alcohols and phenolic compounds, while an absorption band at 2,929 cm^{-1} due to –C-H stretching indicated an alkane group. The two absorptions recorded at 1384 cm^{-1} and 1595 cm^{-1} are due to C-H and N-H stretching, indicating aldehyde and amine groups. And an absorption band at 1121 cm^{-1} due to –C-O stretch, indicating strong alcohol stretching vibrations [32-38].

The FTIR spectrum of biogenic AgNPs exhibited similar FTIR spectral peaks at 1383, 1611, 2925, and 3460 cm-1 (fig. 3b). As a result of the NO_2 symmetric resonances that stretch to nitro compounds, the band at 1383 cm^{-1} suggests C-H vibrations [39]. Peaks at 1,611 cm^{-1} indicate C-C stretching. Further, the peaks at 2,925 caused by aliphatic C-H stretching vibration [40]. The probability of the existence of alcohol in compounds is substantiated by the presence of peaks at 3000 cm^{-1}, indicating a strong intermolecular bond. The O-H stretching shows the highest peak at 3460 cm^{-1} [41, 42]. In previous reports, similar biomolecules were discovered during the synthesis of AgNPs [43]. Compared to the data shown by the synthesized AgNPs

and the plant extracts, these peaks could also be composed of organic materials like proteins and metabolites with functional groups of amines, alcohols, ketones, aldehydes and carboxylic acids. However, the strong broad absorption bands at 3438 cm^{-1}, 1383 cm^{-1}, and 2925 cm^{-1}were attributed to the potential involvement of the functional groups, which were also involved in the reduction of silver nanoparticles [44].

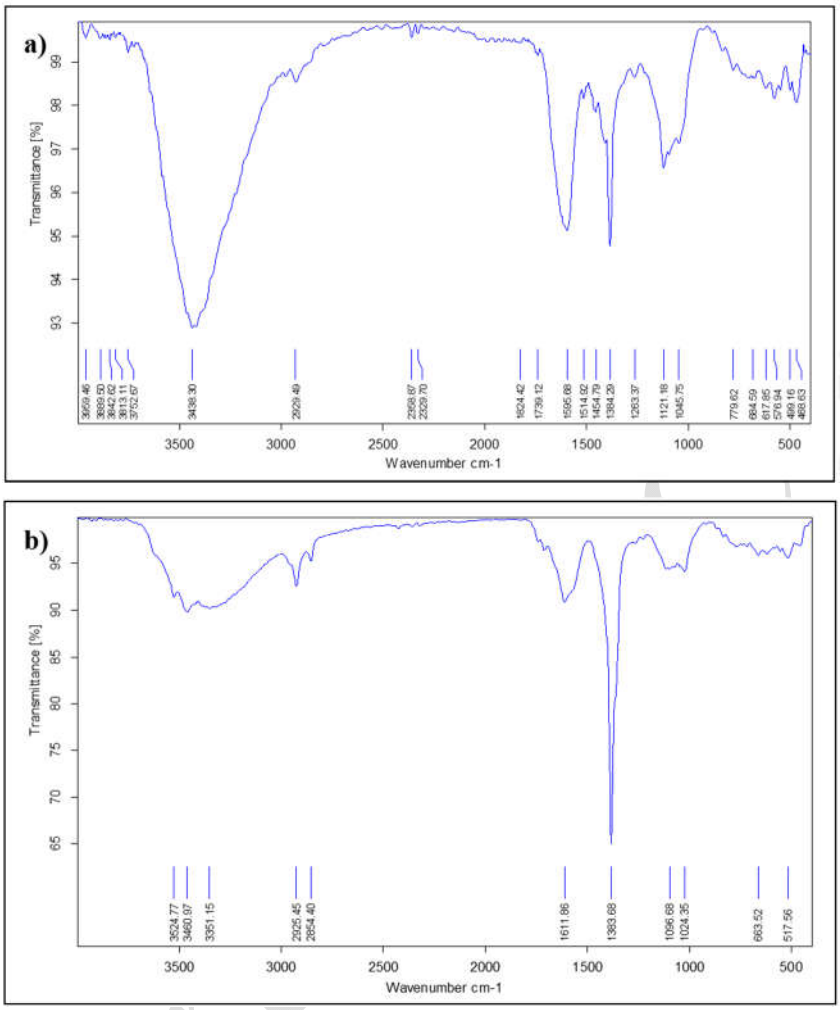

Fig. 3: (a) FTIR spectrum of *Ageratina adenophora* aqueous stem extract. (b) FTIR spectrum of synthesized AgNPs from *Ageratina adenophora* stem extract

X-ray diffraction analysis

To evaluate the crystalline structures of the synthesized AgNPs, XRD analysis was performed. These well-defined XRD patterns showed distinct peaks at 38.03°, 44.06°, 64.37° and 77.34° that correspond to the 111, 200, 220 and 311 crystallographic planes with face-centred cubic structure of metallic silver, respectively (JCPDS No. 04-0783). The average crystalline size was determined by the standard Debye–Scherrer equation. The Bragg's peaks show the arrangement of nanoparticles, and the mean size of the AgNPs was 28.27 nm. The minor background features are attributed to the presence of residual phytochemical compounds from the stem extract. The XRD results (fig. 4) highlight the importance of the stem extracts in shaping the properties of the synthesized AgNPs. The results were compared with the synthesized AgNPs from the *P. alba* leaf extract which showed similar observations reported by Rudrappa *et al.* [45].

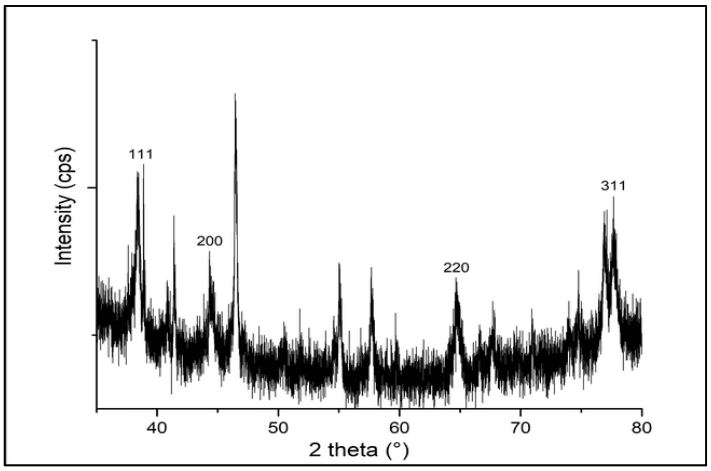

Fig. 4: XRD pattern of synthesized AgNPs from *Ageratina adenophora* stem extract

High-resolution transmission electron microscopy (HR-TEM) analysis

High-resolution transmission electron microscopy (HR-TEM) was used to analyse the synthesized AgNPs particle size, shape, and crystalline nature. TEM investigation showed that the biogenic AgNPs were irregular to spherical in shape, at scale range 50 nm, as shown in fig. 5a and 5b, with particle size in the nano range between 20 to 60 nm with a mean size of 42.1±13.6 nm, respectively (fig. 5c). Similarly, Alshameri *et al.* [46] reported the synthesis of spherical shape AgNPs in the range from 20 nm to 70 nm using *R. nervousus* aqueous leaves extract.

Dynamic light scattering (DLS) analysis

Particle size analysis evaluated the size distribution of biosynthesized AgNPs with an average size range of 115.8 nm with a polydispersity index (PDI) of 0.350, as shown in fig. 5(d). The lower the PDI value (0.7), indicated good quality and the relatively well-defined dimensions of the synthesized AgNPs using *A. adenophora* stem extract. The NPs values of previous studies are different from the values obtained in this study. The disparity in values is likely to be due to the differences in the preparation of the nanoparticles.

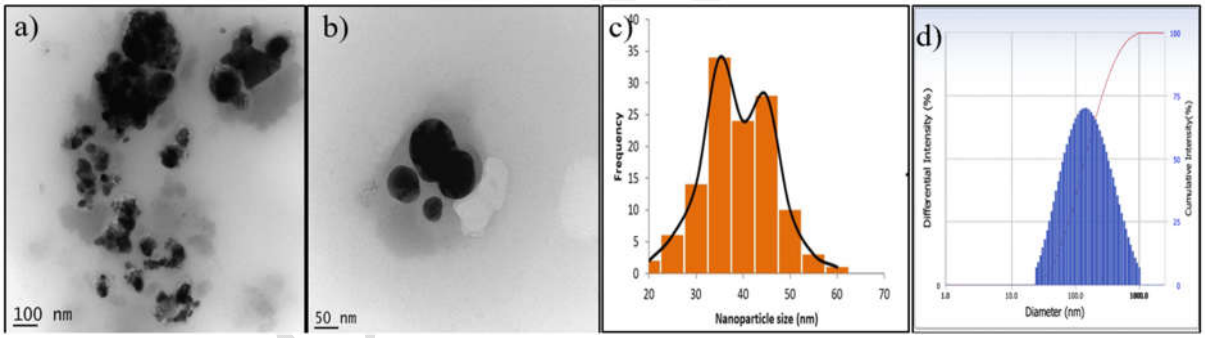

Fig. 5: (a), (b) TEM images showing the morphology of AgNPs in two different magnifications, (c) Histogram showing the size distribution of AgNPs, (d) Particle size distribution by DLS analysis

Qualitative phytochemical analysis

The stem extract of *A. adenophora* yielded flavonoids, saponins, terpenoids, alkaloids, phenols, steroids, proteins, amino acids and sugars as shown in table 1. A slight variation in the secondary metabolite profile was observed with that of earlier reports, which might be due to the variations in the growing conditions across different geographical regions, soil physicochemical and biological parameters [47, 48].

Table 1: Qualitative phytochemical analysis of the aqueous stem extract of *Ageratina adenophora*

Phytochemicals	Aqueous extract
Alkaloids	+
Carbohydrates	+
Flavonoids	+
Glycosides	-
Proteins and amino acids	+
Steroids	+
Phenols	+
Terpenoids	+
Saponins	+
Notes: (+) Sign signifies presence and	(-) Sign signifies non-appearance

Quantitative phytochemical analysis

In this study, the determination of total phenolics, flavonoid and alkaloid content was evaluated to explore the biological significance of the aqueous stem extracts of *A. adenophora*. The stem extract had a total phenol content of 38±0.73 mg/g gallic acid equivalents. The total flavonoid content of 45.16±1.44 mg/g quercetin equivalent, and the total alkaloid content, as determined using the standard curve was 30±0.07, respectively. The alkaloid content was low when compared to the phenol and flavonoid content. The results revealed that the stem extract contains potential amounts of phenolic, flavonoid and alkaloid compounds. According to the previous reports, the determination of total phenolics and flavonoid content of the methanolic extract of the leaves of *A. adenophora* showed that this plant can be one of the potential source of safe natural antioxidants and bioactive components [48]. Further, a detailed examination of these bioactive compounds present in the stem extract is required for the complete evaluation of the individual compounds to understand their different biochemical properties.

Determination of free radical scavenging activity – DPPH assay

The scavenging activity of the biogenic AgNPs with different concentrations 20, 40, 60, 80, and 100 µg was studied by DPPH assay as shown in fig. 6. Ascorbic acid was used as a positive control. The AgNPs showed higher inhibition percent at 100 µg concentration. It also reveals that as the amount of the test sample increased, the free radical scavenging rate also increased. The IC_{50} values, indicating the concentration necessary to block 50% of DPPH radicals, were determined to be 99.08 µg/ml. Accordingly, a previous report by Rajamanikandan *et al.* [23] has stated that the antioxidant activity of AgNPs against different concentrations, with the visual monitoring of the reaction was noticed by the gradual change of colour from dark purple to yellow, which enhanced good antioxidant activity [49, 50].

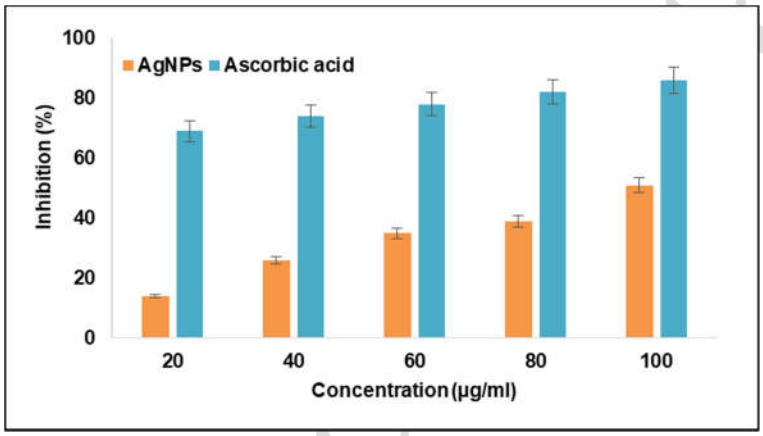

Fig. 6: Antioxidant activity of synthesized AgNPs, values are given as mean±SD for each concentration (n=3)

Antibacterial activity of synthesized AgNPs

The antibacterial effectiveness of biogenic AgNPs against the bacterial culture showed significant inhibitory activity, as shown in table 3. Among the tested pathogens, *S. aureus* showed the largest zone of inhibition, measuring 19.9±0.13 mm, whereas *E. coli* showed the lowest ZOI, measuring 15.0±0.20 mm, as shown in fig. 7. Gentamicin used as a positive control had a strong bactericidal activity. The aqueous stem extract of *A. adenophora* showed some activity for *E. coli* and *S. aureus*. An effective antibacterial activity of AgNPs against bacterial strains demonstrated a similar effect when compared to positive showing prominent activity against infection. However, the present results obtained from the evaluation of the minimum inhibitory concentration against bacterial strains in 24 h are shown in table 2. The MIC against *S. aureus* was 5.5±0.70 µg/ml, 8±0.8 µg/ml for *P. aeruginosa* followed by 7.3±0.45 µg/ml against *B. subtilis* and 8.7±0.05 µg/ml for *E. coli*. However, some previous reports evaluated Gram-negative bacterial strains such as *E. coli* and *P. aureginosa,* which showed lower MIC values when compared to results obtained in this study [51].

Table 2: Antibacterial activity of synthesized AgNPs

S. No.	Microorganisms	ZOI (mm in diameter)		Plant extract	AgNPs	MIC of AgNPs (µg/ml)
		Positive control	$AgNO_3$			
1	*Bacillus subtilis*	24.8±0.15	-	-	19.1±0.13	7.3±0.45
2	*Escherichia coli*	26.0±0.03	11.9±0.07	9.9±0.13	15.0±0.20	8.7±0.05
3	*Staphylococcus aureus*	22.9±0.06	10.0±0.03	15.0±0.7	19.9±0.13	5.5±0.70
4	*Pseudomonas aeruginosa*	24.9±0.12	-	-	18.8±0.12	8±0.8

Note: AgNPs, $AgNO_3$, Plant extract-80 µl concentration, Positive control-20 µl concentration Abbreviations: AgNPs-Silver nanoparticles; AgNO3-Silver nitrate; Plant extract-*A. adenophora* stem extract, Positive control – Gentamycin; ZOI-Zone of inhibition in mm (means of triplicate±standard deviation) and MIC-minimum inhibitory concentration in µg/ml

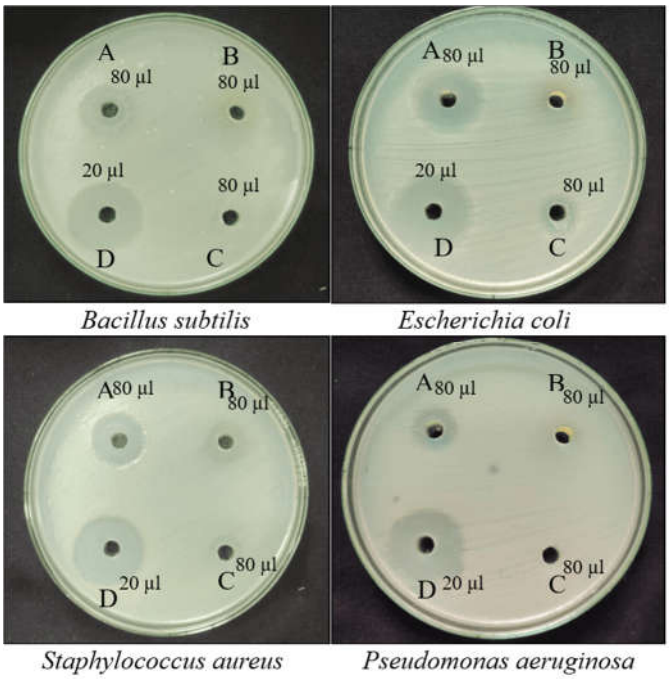

Fig. 7: Antibacterial activity of synthesized AgNPs, Notes: (A) Biogenic AgNPs (B) Aqueous stem extract (C) Silver nitrate (D) Positive control-Gentamycin

Antifungal activity of synthesized AgNPs

The antifungal activity was studied using the well diffusion method of two different fungal strains, *Aspergillus niger* and *Candida albicans*. Among the two fungal pathogens, *C. albicans* was highly sensitive to synthesized AgNPs, 11.9±0.13 mm zone of inhibition, followed by *A. niger* of 10.0±0.03 mm. $AgNO_3$ and plant extract showed the least activity, as shown in fig. 8. The positive control clotrimazole showed higher antifungal activity, yet biogenic AgNPs were discovered to have comparably similar activity to that of the positive control, as shown in table 3. According to the previous report, Bishoyi *et al.* have stated similar fungicide properties of AgNPs against different strains [7, 36].

Table 3: Antifungal activity of synthesized AgNPs

S. No.	Microorganisms	ZOI (mm in diameter)		Plant extract AgNPs	
		Positive control	$AgNO_3$		
1	*Aspergillus niger*	13.8±0.15	8.9±0.06	7.9±0.07	10.0±0.03
2	*Candida albicans*	14.0±0.03	8.9±0.12	-	11.9±0.13

Note: AgNPs, $AgNO_3$, Plant extract-80 µl concentration, Positive control-20 µl concentration Abbreviations: AgNPs-Silver nanoparticles; AgNO3-Silver nitrate; Plant extract-*A. adenophora* stem extract, Positive control – Clotrimazole; ZOI = Zone of inhibition in mm (means of triplicate±standard deviation)

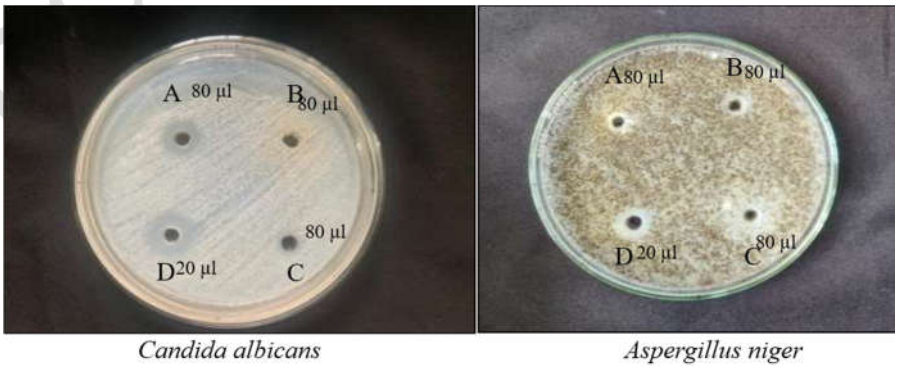

Fig. 8. Antifungal activity of synthesized AgNPs, Notes: (A) Biologically synthesized AgNPs (B) Aqueous stem extract (C) Silver nitrate (D) Positive control-Clotrimazole

***In vitro* cytotoxicity of synthesized AgNPs**

The MTT assay was performed to examine the cytotoxic and cell viability effects of synthesized AgNPs on the Vero cell line. In the present investigation, the AgNPs treated Vero cells demonstrated concentration-dependent cell viability, where low concentration maintained acceptable biocompatibility, and with an increase in AgNP concentration (20, 40, 60, 80, and 100 µg/ml) reduction in cell viability was seen with distinct morphological changes when compared to control cells. The IC_{50} value for Vero cells was recorded at 108.61 µg/ml, respectively, at 24 h (fig. 9). The present study, compared with previous reports using the MTT assay to examine the cytotoxic impact, has shown a low inhibitory effect on the growth of Vero cells, indicating concentration-dependent toxicity of the biosynthesized AgNPs [49, 52].

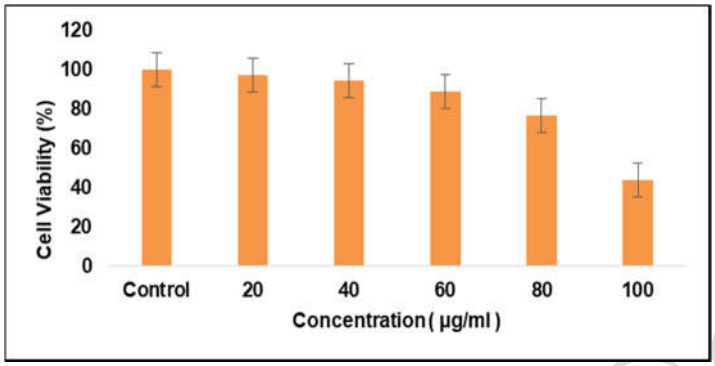

Fig. 9: (A) Cell viability (%) of different concentrations of biosynthesized AgNPs on Vero cell line (20, 40, 60, 80, and 100 µg/ml) by MTT assay, (n=3 values are given as mean±SD)

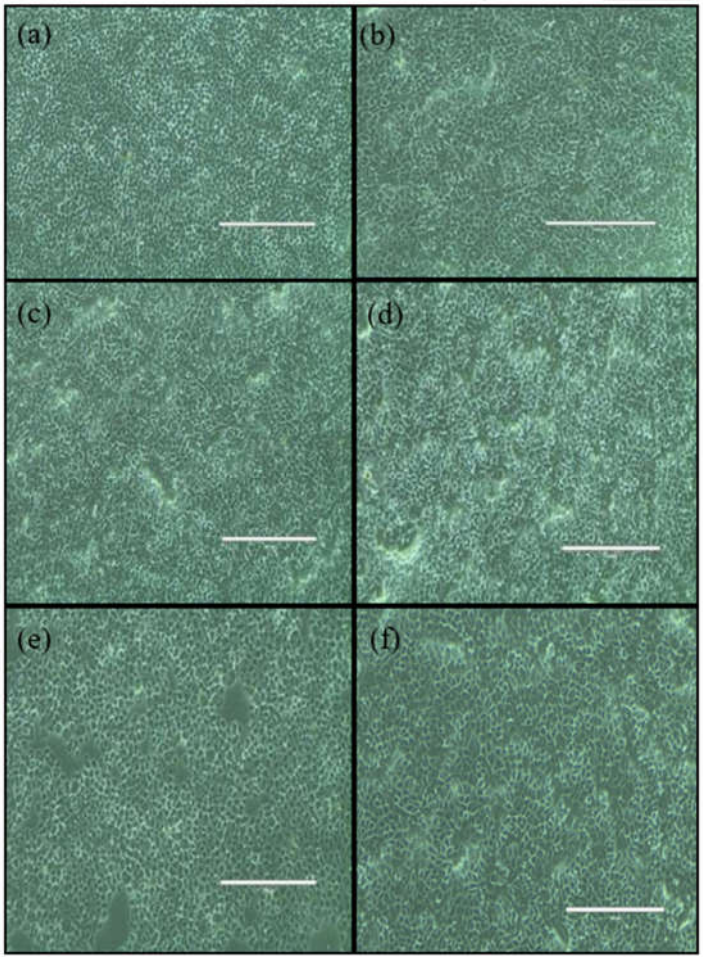

Fig. 9: (B) Cytotoxic effect of biosynthesized AgNPs on Vero cell line. Morphological changes in treated cells with different concentrations of AgNPs (a) 20, (b) 40, (c) 60, (d) 80, (e) 100 µg/ml and (f) Morphological changes in untreated cells (control), respectively

***In vitro* wound healing activity of synthesized AgNPs**

The wound healing activity of the synthesised AgNPs was studied under an inverted microscope, and the percentage rate of the wound healed was calculated. Based on the result obtained at 24 h (18.47%), 48 h (30.43%) and 72 h (57.97%), wound healing was shown to be more effective with

AgNPs significantly accelerated the wound healing process as compared to the negative control group 24 h (11.48 %), 48 h (25.55%), 72 h (36.29%), as shown in fig. 10. The healed cells resembled normal healthy cells, thus showed a positive healing potential. On the other hand, no significant effects were observed after 72 h. Cipladine used as a positive control showed a higher healing rate compared to treated cells. According to previous studies, Ebeling S *et al.* stated that antioxidant and antibacterial activities appear to have beneficial effects on wound healing. Cell migration supported cellular movement, which plays a critical part in the process of wound healing [53]. Kithiyon *et al.* [54] reported the wound healing efficacy of the mycosynthesised AgNPs from *E. scabrosa* with a similar concentration when compared with commercial drug. Thus, it was inferred that biogenic AgNPs have significant wound healing potential.

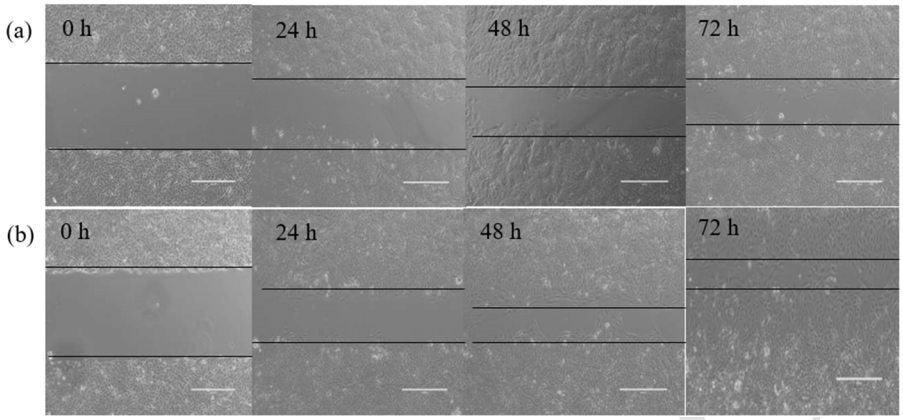

Fig. 10: *In vitro* wound scratch assay (a) Wounded cells (untreated) at different intervals and (b) AgNPs-treated cells at different time intervals (0 h, 24 h, 48 h, 72 h)

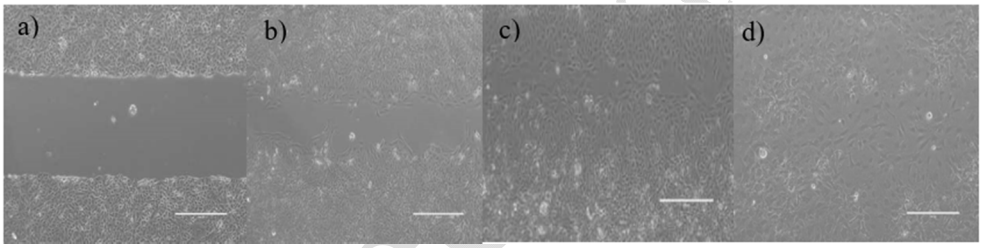

Fig. 11: *In vitro* wound scratch assay (a) Wounded cells, (b) untreated cells, (c) AgNPs treated cells, (d) Commercial drug treated cells

DISCUSSION

The present study demonstrated the successful green synthesis of silver nanoparticles (AgNPs) using the aqueous stem extract of *Ageratina adenophora*. The biological applications of the AgNPs are highly promising. The structural properties were studied by HR-TEM, DLS and XRD analysis. According to previous reports, the peak observed at 410 to 455 nm is attributed to the Surface Plasmon Resonance (SPR) peak of spherical-shaped AgNPs. Previous reports on green synthesized AgNPs have shown peaks at similar positions with good stability. Kowsalya *et al.* reported that *V. vinifera* extract showed good stability for biosynthesis of AgNPs, which strongly supports our result [25]. TEM analysis revealed irregular to spherical in shape of the nanoparticles with a size range of 20 to 60 nm, while XRD analysis confirmed the crystalline nature of the synthesized nanoparticles. The results were compared with Yarrappagaari *et al.* findings obtained for the XRD pattern that showed evidence of diffraction peaks at 111, 200, 220, and 311 at 2θ angles [55]. The average crystalline size calculated from XRD was a smaller particle size of 28.27 nm compared to that observed in TEM images. According to the DLS test, the particles were 115.8 nm in size and showed a narrow distribution with a polydispersity index (PDI) of 0.350. The lower PDI value (0.7) indicated good quality of particles suitable for predictable reactions with tissues and cell walls in the body. Since the properties of nanoparticles vary from formulation to formulation, it highlights the need for careful optimization methods during nano formulations [17]. Thus, the FTIR peaks indicated the presence of amine, hydroxyl and phenolic groups that acted as stabilizing and capping agents, supporting stable nanoparticle formation. In addition, flavonoid being the key phytochemical in the stem extract highlights the significant free radical scavenging properties. These results agree with earlier reports that the AgNPs exhibited significant bioactivities such as antibacterial, antifungal and antioxidant activity. Highlighting the fact that AgNPs are surrounded by a thin layer of organic molecules, which play the role of phytochemicals as capping ligands. Maheswari *et al.* reported ethanol and aqueous extract of *A. adenophora* to exhibit higher scavenging activity, which might be attributed to the presence of polyphenolic compounds and flavonoids [21]. The potential antimicrobial properties shown by AgNPs can therefore be attributed to their morphological size and shape, along with surface chemistry, as these properties are vital during the interaction of NPs with microbial cells. In accordance with the findings of our results, earlier investigations by MosaChristas *et al.* reported antibacterial activity of *M. calabura* methanol leaf extract with similar concentrations by evaluating the minimum inhibitory concentration against pathogenic Gram-negative and Gram-positive bacterial strains [50]. In addition, the AgNPs formed also showed concentration-dependent toxicity on Vero cell line at higher concentrations. The results of our wound scratch assay prove that the biosynthesized AgNPs possess enhanced wound healing properties. Our results correlate with the study of Veeraraghavan *et al.* [57], where the wound healing property of Sb-AgNP with two different concentrations decreased the migration of L929 fibroblast cells and thereby reduced the size of the wound created. Thus, these findings align with previous literature on plant-mediated silver nanoparticles, emphasizing the safety of biologically synthesized nanomaterials.

CONCLUSION

In conclusion, the biosynthesized silver nanoparticles (AgNPs) from *Ageratina adenophora* stem are an eco-friendly approach to form bioactive materials that support future pharmacological and therapeutic applications, particularly in treating infected wounds, highlighting their potential as promising agents in biogenic nanomedicine. A thorough investigation to better understand the mechanism of action *in vivo* is needed. Besides, a further study is aimed at exploring *in vivo* chronic wound infection and also to improve the cell regeneration processes to reduce the side effects.

ACKNOWLEDGEMENT

The authors express their appreciation for the encouragement and support provided by the Principal and Head of Department, Department of Plant Biology and Biotechnology, Loyola College, to undertake this research. We would like to thank The Director, AviGen Bio Pvt. Ltd., Chennai, for providing the laboratory facilities, CLRI-CATERS-Chennai, SAIF-STIC, Kochi and CSIR-CECRI, Karaikudi for providing the instrumentation facility for characterization analyses.

FUNDING

This research did not receive any specific grant from funding agencies in the public, commercial, or not-for-profit sectors.

AUTHORS CONTRIBUTIONS

Lishanthi Ravi: Conceptualization, Investigation, Methodology, Validation, Formal analysis, Data curation, Writing – original draft. Lorraine V Mary Rocha: Investigation, Methodology, Validation, Data curation. Madeena S Begum: Methodology and Data curation. A Hadsun Jona: Methodology and Validation. Jaquline Chinna Rani I: Conceptualization, Methodology, Supervision and writing – review and editing. All authors have approved the final version of the manuscript.

CONFLICTS OF INTERESTS

The authors report no conflicts of interest in performing this work

REFERENCES

1. Bapat MS, Singh H, Shukla SK, Singh PP, Vo DN, Yadav A. Evaluating green silver nanoparticles as prospective biopesticides: an environmental standpoint. Chemosphere [ePub]. 2022 Jan;286(2):131761. doi: 10.1016/j.chemosphere.2021.131761, PMID 34375828.
2. Das SK, Khan MM, Guha AK, Das AR, Mandal AB. Silver-nano biohybride material: synthesis, characterization and application in water purification. Bioresour Technol. 2012 Nov;124:495-9. doi: 10.1016/j.biortech.2012.08.071 [ePub]. PMID 23021961.
3. Ansari M, Ahmed S, Abbasi A, Khan MT, Subhan M, Bukhari NA et al. Plant mediated fabrication of silver nanoparticles, process optimization, and impact on tomato plant. Sci Rep. 2023 Oct 23;13(1):18048. doi: 10.1038/s41598-023-45038-x, PMID 37872286, PMCID PMC10593853.
4. Rizwana H, Aljowaie RM, Al Otibi F, Alwahibi MS, Alharbi SA, Al Asmari SA et al. Antimicrobial and antioxidant potential of the silver nanoparticles synthesized using aqueous extracts of coconut meat (Cocos nucifera L). Sci Rep. 2023 Sep 27;13(1):16270. doi: 10.1038/s41598-023-43384-4, PMID 37758773, PMCID PMC10533512.
5. Singh P, Pandit S, Beshay M, Mokkapati VR, Garnaes J, Olsson ME et al. Anti-biofilm effects of gold and silver nanoparticles synthesized by the Rhodiola rosea rhizome extracts. Artif Cells Nanomed Biotechnol. 2018;46 sup3:S886-99. doi: 10.1080/21691401.2018.1518909 [ePub]. PMID 30422688.
6. Swarnalatha M, Ragunathan R, Johney J, Vishnupriya R. Biogenic synthesis of silver nanoparticles using *Chromolaena odorata* leaf extract and its antioxidant, antimicrobial, and anticancer activities. J Environ Nanotechnol. 2024;13(4):27-35. doi: 10.13074/jent.2024.12.243876.
7. Bishoyi AK, Sahoo CR, Samal P, Mishra NP, Jali BR, Khan MS et al. Unveiling the antibacterial and antifungal potential of biosynthesized silver nanoparticles from Chromolaena odorata leaves. Sci Rep. 2024 Mar 29;14(1):7513. doi: 10.1038/s41598-024-57972-5, PMID 38553574, PMCID PMC10980689.
8. Das G, Patra JK, Shin HS. Biosynthesis, and potential effect of fern mediated biocompatible silver nanoparticles by cytotoxicity, antidiabetic, antioxidant and antibacterial, studies. Mater Sci Eng C Mater Biol Appl. 2020 Sep;114:111011. doi: 10.1016/j.msec.2020.111011 [ePub]. PMID 32993988.
9. Ajitha B, Ashok Kumar Reddy Y, Sreedhara Reddy P. P. Green synthesis and characterization of silver nanoparticles using Lantana camara leaf extract. Mater Sci Eng C Mater Biol Appl. 2015 Apr;49:373-81. doi: 10.1016/j.msec.2015.01.035 [ePub]. PMID 25686962.
10. Wan F, Liu W, Guo J, Qiang S, Li B, Wang J et al. Invasive mechanism and control strategy of Ageratina adenophora (Sprengel). Sci China Life Sci. 2010 Nov;53(11):1291-8. doi: 10.1007/s11427-010-4080-7 [ePub]. PMID 21046320.
11. Sun W, Liu SS, Zhao CC. Biological properties of active compounds from *Ageratina adenophora*. Sage Open Med. 2023 May 15;11:20503121231167964. doi: 10.1177/20503121231167964, PMID 37205157, PMCID PMC10186572.
12. Dua TK, Giri S, Nandi G, Sahu R, Shaw TK, Paul P. Green synthesis of silver nanoparticles using *Eupatorium adenophorum* leaf extract: characterizations, antioxidant, antibacterial and photocatalytic activities. Chem Zvesti. 2023;77(6):2947-56. doi: 10.1007/s11696-023-02676-9 [ePub]. PMID 36714039, PMCID PMC9873543.
13. Poudel R, Neupane NP, Mukeri IH, Alok S, Verma A. An updated review on invasive nature, phytochemical evaluation, and pharmacological activity of *Ageratina adenophora*. Int J Pharm Sci Res. 2020;11(6):2510-20. doi: 10.13040/IJPSR.0975-8232.11(6).2510-20.
14. Balashanmugam P, Kalaichelvan PT. Biosynthesis characterization of silver nanoparticles using Cassia roxburghii DC. Aqueous extract, and coated on cotton cloth for effective antibacterial activity. Int J Nanomedicine. 2015 Oct 1;10 Suppl 1:87-97. doi: 10.2147/IJN.S79984. PMID 26491310, PMCID PMC4599608.
15. Habibullah G, Viktorova J, Ulbrich P, Ruml T. Effect of the physicochemical changes in the antimicrobial durability of green synthesized silver nanoparticles during their long-term storage. RSC Adv. 2022 Oct 25;12(47):30386-403. doi: 10.1039/d2ra04667a, PMID 36349158, PMCID PMC9594854.
16. PULIPAKA S, SUTTEE A, VANI R, JYOTHI V. Green synthesis of zinc oxide nanoparticles of Tradescantia spathacea plant. Int J Appl Pharm. 2025;18(1):272-82. doi: 10.22159/ijap.2026v18i1.55297.
17. PAGAR SA, THOMBRE NA. Development and optimization of mesoporous silica nanoparticles loaded with Adiantum Philippines fraction and thuja oil as a potential wound healing agent. Int J Appl Pharm. 2026;18(1):141-54. doi: 10.22159/ijap.2026v18i1.55787.
18. Paramasivam D, Balasubramanian B, Suresh R, Kumaravelu J, Vellingiri MM, Liu WC et al. One-pot synthesis of silver nanoparticles derived from aqueous leaf extract of *Ageratum conyzoides* and their biological efficacy. Antibiotics (Basel). 2023 Apr 1;12(4):688. doi: 10.3390/antibiotics12040688, PMID 37107050, PMCID PMC10135330.
19. Ramakrishna A, Ravishankar GA. Influence of abiotic stress signals on secondary metabolites in plants. Plant Signal Behav. 2011 Nov;6(11):1720-31. doi: 10.4161/psb.6.11.17613 [ePub]. PMID 22041989, PMCID PMC3329344.
20. Siddiqui M. Phytochemical analysis of some medicinal plants. lmrj. 2021;3(8):1-5. doi: 10.38106/lmrj.2021.36.

21. Maheswari B L, Mani N MN, Kavikala N KN, Karthika S KS, Rajasudha RV. Evaluation of secondary metabolites of *Ageratina adenophora* and synthesis of silver nanoparticles for its antibacterial and antioxidant activity. Orient J Chem. 2023;39(1):102-13. doi: 10.13005/ojc/390112.
22. Tabasum S, Khare S, Jain K. Spectrophotometric quantification of total phenolic, flavonoid, and alkaloid contents of abrus precatorius L. Seeds. Asian J Pharm Clin Res. 2016;9:371-4.
23. Rajamanikandan S, Sindhu T, Durgapriya D, Sophia D, Ragavendran P, Gopalakrishnan VK. Radical scavenging and antioxidant activity of ethanolic extract of Mollugo nudicaulis by *in vitro* assays. Indian J Pharm Educ Res. 2011;45(4):310-6.
24. SARVARAIDU CH, ALI M. *In vitro* antioxidant and molecular docking studies for anti-Alzheimer potential of ethanolic extract of Alternanthera sessilis and lantana Camara. Asian J Pharm Clin Res. Nov 2025;18(11):164-73. doi: 10.22159/ajpcr.2025v18i11.55639.
25. E K, K M, P B, A TS, I JC. Biocompatible silver nanoparticles/poly(vinyl alcohol) electrospun nanofibers for potential antimicrobial food packaging applications. Food Packag Shelf Life. 2019;21:100379. doi: 10.1016/j.fpsl.2019.100379.
26. Balashanmugam P, Durai P, Balakumaran MD, Kalaichelvan PT. Phytosynthesized gold nanoparticles from C. roxburghii DC. leaf and their toxic effects on normal and cancer cell lines. J Photochem Photobiol B. 2016 Dec;165:163-73. doi: 10.1016/j.jphotobiol.2016.10.013 [ePub]. PMID 27855358.
27. Mosmann T. Rapid colorimetric assay for cellular growth and survival: application to proliferation and cytotoxicity assays. J Immunol Methods. 1983 Dec 16;65(1-2):55-63. doi: 10.1016/0022-1759(83)90303-4, PMID 6606682.
28. Younis NS, Mohamed ME, El Semary NA. Green synthesis of silver nanoparticles by the Cyanobacteria *Synechocystis* sp.: characterization, antimicrobial and diabetic wound-healing actions. Mar Drugs. 2022 Jan 6;20(1):56. doi: 10.3390/md20010056, PMID 35049911, PMCID PMC8781738.
29. Felice F, Zambito Y, Belardinelli E, Fabiano A, Santoni T, Di Stefano R. Effect of different chitosan derivatives on *in vitro* scratch wound assay: a comparative study. Int J Biol Macromol. 2015 May;76:236-41. doi: 10.1016/j.ijbiomac.2015.02.041 [ePub]. PMID 25748846.
30. Noginov MA, Zhu G, Bahoura M, Adegoke J, Small C, Ritzo BA, et al. The effect of gain and absorption on surface plasmons in metal nanoparticles. Appl Phys B. 2007;86(3):455-60. doi: 10.1007/s00340-006-2401-0.
31. Oluwaniyi OO, Adegoke HI, Adesuji ET, Alabi AB, Bodede SO, Labulo AH, et al. Biosynthesis of silver nanoparticles using aqueous leaf extract of *Thevetia peruviana* Juss and its antimicrobial activities. Appl Nanosci. 2016;6(6):903-12. doi: 10.1007/s13204-015-0505-8.
32. Khane Y, Benouis K, Albukhaty S, Sulaiman GM, Abomughaid MM, Al Ali A et al. Green synthesis of silver nanoparticles using aqueous *Citrus limon* zest extract: characterization and evaluation of their antioxidant and antimicrobial properties. Nanomaterials (Basel). 2022 Jun 10;12(12):2013. doi: 10.3390/nano12122013, PMID 35745352, PMCID PMC9227472.
33. Kowsalya E, MosaChristas K, Jaquline CR, Balashanmugam P, Devasena T. Gold nanoparticles induced apoptosis via oxidative stress and mitochondrial dysfunctions in MCF-7 breast cancer cells. Applied Organom Chemis. 2021;35(1):e6000. doi: 10.1002/aoc.6071.
34. Vinodhini S, Vithiya BS, Prasad TA. Green synthesis of palladium nanoparticles using aqueous plant extracts and its biomedical applications. J King Saud Univ Sci. 2022;34(4):102017. doi: 10.1016/j.jksus.2022.102017.
35. Pérez-Marroquín XA, Aguirre-Cruz G, Campos-Lozada G, Callejas-Quijada G, León-López A, Campos-Montiel RG et al. Green synthesis of silver nanoparticles for preparation of gelatin films with antimicrobial activity. Polymers (Basel). 2022 Aug 24;14(17):3453. doi: 10.3390/polym14173453, PMID 36080528, PMCID PMC9460488.
36. Siddiqui M, Giri S, Sahu R, Paul P, Nandi G, Dua TK, et al. Antibacterial and antifungal activity of functionalized cotton fabric with nanocomposite based on silver nanoparticles and carboxymethyl chitosan. Appl Environ Microbiol. 2022;88(3):e02306-21. doi: 10.1128/AEM.02306-21.
37. Motta A, Maniglio D, Migliaresi C, Kim HJ, Wan X, Hu X et al. Silk fibroin processing and thrombogenic responses. J Biomater Sci Polym Ed. 2009;20(13):1875-97. doi: 10.1163/156856208X399936, PMID 19793445.
38. Sajjad A, Ali H, Zia M. Fabrication and evaluation of vitamin doped ZnO/AgNPs nanocomposite based wheat gluten films: a promising findings for burn wound treatment. Sci Rep. 2023 Sep 26;13(1):16072. doi: 10.1038/s41598-023-43413-2, PMID 37752271, PMCID PMC10522583.
39. Parveen M, Ahmad F, Malla AM, Azaz S. Microwave-assisted green synthesis of silver nanoparticles from *Fraxinus excelsior* leaf extract and its antioxidant assay. Appl Nanosci. 2016;6(2):267-76. doi: 10.1007/s13204-015-0433-7.
40. Supraja S, Mohammed AS, Chakravarthy N, Priya AJ, Sagadevan E, Kasinathan MK, et al. Green synthesis of silver nanoparticles from Cynodon dactylon leaf extract. Int J ChemTech Res. 2013;5(1):271-7.
41. Rajashekar A, Janakiraman V, Govindarajan K. *In vitro* cytotoxic study of green synthesized gold and silver nanoparticles using Eclipta prostrata (L.) against HT-29 cell line. Asian J Pharm Clin Res. 2016;9(5):189-93. doi: 10.22159/ajpcr.2016.v9i5.13194.
42. Moon JY, Lee J, Hwang TI, Park CH, Kim CS. A multifunctional, one-step gas foaming strategy for antimicrobial silver nanoparticle-decorated 3D cellulose nanofiber scaffolds. Carbohydr Polym. 2021 Dec 1;273:118603. doi: 10.1016/j.carbpol.2021.118603 [ePub]. PMID 34561003.
43. Saranyaadevi K, Subha V, Ernest Ravindran RS, Renganathan S. Green synthesis and characterization of silver nanoparticle using leaf extract of Capparis zeylanica. Asian J Pharm Clin Res. 2014;2(SUPPL. 2);7(SUPPL.:44-8.
44. Alkhalaf MI, Hussein RH, Hamza A. Green synthesis of silver nanoparticles by *Nigella sativa* extract alleviates diabetic neuropathy through anti-inflammatory and antioxidant effects. Saudi J Biol Sci. 2020 Sep;27(9):2410-9. doi: 10.1016/j.sjbs.2020.05.005 [ePub]. PMID 32884424, PMCID PMC7451673.
45. Rudrappa M, Rudayni HA, Assiri RA, Bepari A, Basavarajappa DS, Nagaraja SK et al. *Plumeria alba*-mediated green synthesis of silver nanoparticles exhibits antimicrobial effect and anti-oncogenic activity against glioblastoma U118 MG cancer cell line. Nanomaterials (Basel). 2022 Jan 30;12(3):493. doi: 10.3390/nano12030493, PMID 35159838, PMCID PMC8839720.
46. Alshameri AW, Owais M, Altaf I, Farheen SS. Rumex nervosus mediated green synthesis of silver nanoparticles and evaluation of its *in vitro* antibacterial, and cytotoxic activity. OpenNano. 2022;8:100084. doi: 10.1016/j.onano.2022.100084.
47. Poudel R, Neupane NP, Mukeri IH, Alok S, Verma A. An updated review on invasive nature, phytochemical evaluation, and pharmacological activity of *Ageratina adenophora*. Int J Pharm Sci Res. 2020;11(6):2510-20. doi: 10.13040/IJPSR.0975-8232.11(6).2510-20.
48. Devkota A, Das RK. Phytochemical screening and in-vitro evaluation of antimicrobial activity of invasive species Ageratina adenophora collected from Kathmandu valley, Nepal. Sci World. 2022;15(15):120-6. doi: 10.3126/sw.v15i15.45660.
49. Badmus JA, Oyemomi SA, Adedosu OT, Yekeen TA, Azeez MA, Adebayo EA et al. Photo-assisted bio-fabrication of silver nanoparticles using *Annona muricata* leaf extract: exploring the antioxidant, anti-diabetic, antimicrobial, and cytotoxic activities. Heliyon. 2020 Nov 3;6(11):e05413. doi: 10.1016/j.heliyon.2020.e05413, PMID 33195844, PMCID PMC7644911.
50. MosaChristas K, Kowsalya E, Karthick R, Jaquline CR. Antibacterial, antibiofilm and anti-quorum sensing activities of Muntingia calabura L. Leaf extract against Pseudomonas aeruginosa. Lett Appl Microbiol. 2022 Sep;75(3):588-97. doi: 10.1111/lam.13595 [ePub]. PMID 34725846.
51. Azam A, Ahmed F, Arshi N, Chaman M, Naqvi A. One step synthesis and characterization of gold nanoparticles and their antibacterial activities against E. coli (ATCC 25922 strain). Int J Theor Appl Sci. 2009;1.
52. K. MS, P. B, K. M, A. TS, R. S. *In vitro* cytotoxicity of biosynthesized gold nanoparticles from shells of Pistacia vera L. Int J App Pharm. 2018;10(4):162. doi: 10.22159/ijap.2018v10i4.27154.
53. Ebeling S, Naumann K, Pollok S, Wardecki T, Vidal-Y-Sy S, Nascimento JM, Boerries M, Schmidt G, Brandner JM, Merfort I. From a traditional medicinal plant to a rational drug: understanding the clinically proven wound healing efficacy of birch bark extract. PLoS One. 2014 Jan 22;9(1):e86147. doi: 10.1371/journal. pone.0086147. PMID: 24465925; PMCID: PMC3899119.

54. Kithiyon M, Pannerselvam B, Balasaubramaniyam Madhukumar SS, Sridharan J, Alagumuthu TS. Efficacy of mycosynthesised AgNPs from *Earliella scabrosa* as an *in vitro* antibacterial and wound healing agent. IET Nanobiotechnol. 2019 May;13(3):339-44. doi: 10.1049/iet-nbt.2018.5237, PMID 31053699, PMCID PMC8676610.
55. Yarrappagaari S, Gutha R, Narayanaswamy L, Thopireddy L, Benne L, Mohiyuddin SS et al. Eco-friendly synthesis of silver nanoparticles from the whole plant of *Cleome viscosa* and evaluation of their characterization, antibacterial, antioxidant and antidiabetic properties. Saudi J Biol Sci. 2020 Dec;27(12):3601-14. doi: 10.1016/j.sjbs.2020.07.034 [ePub]. PMID 33304171, PMCID PMC7715480.
56. Veeraraghavan VP, Periadurai ND, Karunakaran T, Hussain S, Surapaneni KM, Jiao X. Green synthesis of silver nanoparticles from aqueous extract of *Scutellaria barbata* and coating on the cotton fabric for antimicrobial applications and wound healing activity in fibroblast cells (L929). Saudi J Biol Sci. 2021 Jul;28(7):3633-40. doi: 10.1016/j.sjbs.2021.05.007 [ePub]. PMID 34220213, PMCID PMC8241602.